Photocatalytic Property of a Decatungstate-Containing Bilayer System for the Conversion of 2-Propanol to Acetone

Isamu Moriguchi, Kouji Orishikida, Yasuo Tokuyama, Hiroaki Watabe, Shuichi Kagawa, and Yasutake Teraoka*

Department of Applied Chemistry, Faculty of Engineering, Nagasaki University, 1-14 Bunkyo-machi, Nagasaki 852-8521, Japan

Received January 3, 2001. Revised Manuscript Received March 30, 2001

A decatungstate-containing bilayer composite was prepared by ion complexation between decatungstate anion (W_{10}) and dioctadecyldimethylammonium (DODMA). The cast film prepared from its chloroform solution had a well-organized bilayer structure and a phase transition of the bilayer. The W_{10}/DODMA composite powder dispersed in 2-propanol photocatalyzed the oxidative dehydrogenation of 2-propanol into acetone in the presence of oxygen and under UV irradiation. The W_{10}/DODMA exhibited a unique temperature-dependent property that the photocatalytic activity is drastically enhanced above the phase-transition temperature of the bilayer. When the W_{10}/DODMA composite was combined with Pt nanoparticles, the photocatalytic dehydrogenation of 2-propanol into acetone and H_2 proceeded in the absence of oxygen because Pt promoted the reoxidation of protonated $H_2W_{10}O_{32}^{4-}$ to the original $W_{10}O_{32}^{4-}$ (H_2 evolution step).

Introduction

Recently, synthesis and application of organic−inorganic nanocomposite systems have been becoming an important field in advanced material science.[1] In particular, a great deal of attention has been devoted to the synthesis and/or assembly of nanosized inorganic materials in organized molecular assemblies (OMAs) such as Langmuir−Blodgett films and bilayers.[2−8] Because the hydrophilic headgroups of OMA-constructing molecules have an ion-binding ability, the amount and the spatial arrangement of inorganic precursor ions or cluster ions are well restricted by the highly ordered and assembled headgroups. Therefore, the hydrophilic interlayers of OMAs are expected to be a spatially and chemically constrained reaction field for size- and shape-controlled synthesis of inorganic nanomaterials and/or their two-dimensional arrangement.

As one of such investigations, polyoxometalate cluster ions with a size around a few nanometers have been assembled two-dimensionally in the hydrophilic interlayers of bilayer[9,10] and a Langmuir−Blodgett film[11,12] via ion complexation to give organic−inorganic nanolayered composites. Inorganic isopolyanions (tungstate, vanadate, molybdate, etc.) and heteropolyanions (molybdophosphate, tungstophosphate, etc.) are well-known to have electrochemical,[13] photochemical,[14] photochromic,[15] and/or catalytic properties.[16] Thus, it is expected that an OMA−polyoxometalate system becomes a unique material in which functions that originated from polyoxometalates and organic molecules are synchronized and/or hybridized at the molecular level.[9,12,17,18] For example, multibilayer films composed of polyoxometalate and bilayer-forming amphiphile possessed a unique electrochemical redox property associated with the phase transition of a bilayer[9] and layer-by-layer assembled films of decatungstate ($W_{10}O_{32}^{4-}$), and the cationic polyelectrolyte showed stable electrochromism.[17]

The present study describes for the first time photocatalytic properties of decatungstate-containing bilayer systems as a candidate of a novel functionalized bilayer system as well as a novel organic−inorganic nanocom-

* To whom correspondence should be addressed: Tel.: +81-95-847-1111 (ext. 2737). Fax: +81-95-848-9652. E-mail: yasu@net.nagasaki-u.ac.jp.

(1) For example, Fendler, J. H. *Nanoparticles and Nanostructured Films*; Wiley−VCH: Weinheim, 1999. Ozin, G. A. *Adv. Mater.* **1992**, *4*, 612.
(2) Fendler, J. H.; Meldrum, F. C. *Adv. Mater.* **1995**, *7*, 607.
(3) Moriguchi, I.; Matsuo, K.; Sakai, M.; Hanai, K.; Teraoka, Y.; Kagawa, S. *J. Chem. Soc., Faraday Trans.* **1998**, *94*, 2199.
(4) Moriguchi, I.; Hosoi, K.; Nagaoka, H.; Teraoka, Y.; Kagawa, S. *J. Chem. Soc., Faraday Trans.* **1994**, *90*, 349.
(5) Moriguchi, I.; Tanaka, I.; Teraoka, Y.; Kagawa, S. *J. Chem. Soc., Chem. Commun.* **1991**, 1401.
(6) Pike, J. K.; Byrd, H.; Morone, A. A.; Talham, D. R. *J. Am. Chem. Soc.* **1993**, *115*, 8497.
(7) Kimizuka, N.; Miyoshi, T.; Ichinose, I.; Kunitake, T. *Chem. Lett.* **1991**, 2039.
(8) Moriguchi, I.; Shibata, F.; Teraoka, Y.; Kagawa, S. *Chem. Lett.* **1995**, 761.
(9) Moriguchi, I.; Hanai, K.; Hoshikuma, A.; Teraoka, Y.; Kagawa, S. *Chem. Lett.* **1994**, 691.
(10) Ichinose, I.; Asai, T.; Yoshimura, S.; Kimizuka, N.; Kunitake, T. *Chem. Lett.* **1994**, 1837.
(11) Clemente-Leon, M.; Agricole, B.; Mingotaud, C.; Gomez-Garcia, C. J.; Coronado, E.; Delhaes, P. *Ang. Chem. Int. Ed. Eng.* **1997**, *36*, 1114.
(12) Coronado, E.; Mingotaud, C. *Adv. Mater.* **1999**, *11*, 869.
(13) Sadakane, M.; Steckhan, E. *Chem. Rev.* **1998**, *98*, 219.
(14) Yamase, T. *Chem. Rev.* **1998**, *98*, 307.
(15) Katsoulis, D. E. *Chem. Rev.* **1998**, *98*, 359.
(16) Mizuno, M.; Misono, M. *Chem. Rev.* **1998**, *98*, 199.
(17) Moriguchi, I.; Fendler, J. H. *Chem. Mater.* **1988**, *10*, 2205.
(18) Volkmer, D.; Chesne, A. D.; Kurth, D. G.; Schablegger, H.; Lehmann. P.; Koop, M. J.; Muller, A. *J. Am. Chem. Soc.* **2000**, *122*, 1995.

10.1021/cm010007v CCC: $20.00
Published on Web 06/07/2001

posite. The preparation and structural characterization of decatunstate-containing bilayer systems were also described.

Experimental Section

Materials. Dioctadecyldimethylammonium bromide (DODMA·Br) and tetrabutylammonium bromide (TBA·Br) were obtained from Tokyo Kasei Ind. Ltd. (extra-pure grade) and were used as received. All the other chemicals (potassium hexachloroplatinate, sodium tungstate 2-hydrate, chloroform, 2-propanol, ethanol, and 35 wt % aqueous solution of formaldehyde) were guaranteed reagents (Kishida Chemical. Ltd.). An aqueous solution of decatungstate anion ($W_{10}O_{32}^{4-}$) was prepared by the acidification of 0.1 M (1 M = 1 mol·dm^{-3}) aqueous Na_2WO_4 to pH 2 by the dropwise addition of aqueous HCl under vigorous stirring.[19] The formation of $W_{10}O_{32}^{4-}$ in the aqueous phase was identified by its characteristic absorption maximum around 323 nm of the oxygen-to-tungsten charge-transfer band.[20] Water used was purified by using a Millipore Milli-Q filter system (resistivity >14 MΩ).

Synthesis of Ion Complexes between Cationic Amphiphiles and $W_{10}O_{32}^{4-}$ or $PtCl_6^{2-}$. Quaternary alkylammonium compound (DODMA·Br, TBA·Br) (1.6 mmol) was dispersed in 100 mL of water (pH 2) by sonication, and then 100 mL of aqueous $W_{10}O_{32}^{4-}$ (4 mM, pH 2) was added to the solution under vigorous stirring; the molar mixing ratio of [quaternary alkylammonium]/[$W_{10}O_{32}^{4-}$] was 4. The precipitates, which were produced immediately by mixing these aqueous solutions, were collected by filtration, washed with water, and dried in a vacuum. The obtained ion complexes were denoted as W_{10}/DODMA and W_{10}/TBA in the following. Similarly, an ion complex of $PtCl_6^{2-}$/DODMA was prepared from mixing the aqueous solution of DODMA and aqueous $PtCl_6^{2-}$ with the molar ratio of [DODMA]/[$PtCl_6^{2-}$] = 2.

Synthesis of Composite Consisting of DODMA, $W_{10}O_{32}^{4-}$, and Pt Nanoparticles. The ion complex of $PtCl_6^{2-}$/DODMA (0.3 mmol) was dissolved in 80 mL of chloroform and the solution was refluxed at 80 °C in the presence of 0.5 mL of 37 wt % formaldehyde and 2.5 mmol of sodium hydroxide under atmospheric N_2.[21] After the mixture was refluxed for 2 h, a clear and dark brown solution was produced. The solution was mixed with 200 mL of water, and then the organic phase was extracted and evaporated to yield black powder. The obtained composite was designated Pt/DODMA.

The composites of three components, DODMA, $W_{10}O_{32}^{4-}$, and Pt nanoparticles, were also prepared by dissolving the W_{10}/DODMA and the Pt/DODMA in chloroform with a molar mixing ratio of x (=[Pt]/[$W_{10}O_{32}^{4-}$]) in a range of 0.05−0.7, followed by evaporating the solvent and drying in a vacuum. The composite was denoted as W_{10}/Pt[x]/DODMA.

Analysis. The composites prepared were characterized by elementary analysis, thermogravimetry (Seiko TG/DTA 200), IR measurement (Perkin-Elmer 1650 spectrometer), and X-ray diffraction (XRD) measurement (Rigaku RINT2200 diffractometer, Cu Kα) in the form of powder or film, which was prepared by casting its chloroform solution. IR spectra of the cast film of W_{10}/DODMA (0.5 mg) in 2-propanol were measured by using a liquid cell filled with 10 μL of 2-propanol under controlled temperature (10−45 °C). Differential scanning calorimetry (DSC) (Shimadzu DSC-50) of the W_{10}/DODMA film (2 mg) was carried out in the temperature range of 0−90 °C at a heating rate of 2 °C·min^{-1} with 20 μL of water, ethanol, or 2-propanol.

Photocatalytic Reactions. Photocatalytic dehydrogenation reactions of ethanol and 2-propanol were carried out in a quartz vessel equipped with a condenser between 15 and 45 °C under flowing air or N_2. A 100-W mercury lamp was used as a light source. Typically, 0.1 mmol of the powder of W_{10}/DODMA, Pt/DODMA, or W_{10}/Pt[x]/DODMA was dispersed in 200 mL of degassed alcohol and then air or N_2 gas was bubbled for 30 min prior to the photoillumination. Gas chromatography (Shimadzu GC-8A) was employed for analyses of alcohol, aldehyde, and ketone in the solution (column: BX-10) and hydrogen in the atmospheric N_2 gas phase (column: molecular sieve 5A).

Results and Discussion

Preparation and Structural Characterization of W_{10}/DODMA Ion Complex. The W_{10}/DODMA ion complex, which was prepared by mixing aqueous $W_{10}O_{32}^{4-}$ and aqueous DODMA, showed IR bands of CH stretching around 2800−3000 cm^{-1} due to alkyl chains of DODMA and W−O stretching characteristic of $W_{10}O_{32}^{4-}$ at 957, 897, and 800 cm^{-1}.[22] In addition, the quartz-supported W_{10}/DODMA film exhibited UV absorption peaks of $W_{10}O_{32}^{4-}$ at 323 nm due to the oxygen-to-metal charge-transfer band,[20] substantiating the incorporation of $W_{10}O_{32}^{4-}$ into the composite without any structural alteration. The composition of W_{10}/DODMA was verified by elementary analysis. Found (%): C, 40.10; H, 6.99; N, 1.22. Calcd (%) for $W_{10}O_{32}^{4-}$·$(DODMA^+)_4$: C, 40.08; H, 7.08; N, 1.23. The molar ratio of $W_{10}O_{32}^{4-}$:DODMA in the W_{10}/DODMA ion complex was 1:4, consistent with the value expected from the electric charge balance between them. It was also confirmed by thermogravimetry that the weight loss of W_{10}/DODMA in air up to 550 °C (48.9%) was consistent with the calculated value (48.4%) considering the production of WO_3 from $W_{10}O_{32}^{4-}$·$(DODMA^+)_4$. The W_{10}/TBA ion complex prepared in the same manner also showed W−O stretching IR bands of $W_{10}O_{32}^{4-}$ and possessed the molar ratio of $W_{10}O_{32}^{4-}$:TBA = 1:4.

The W_{10}/DODMA ion complex did not dissolve in water, ethanol, and 2-propanol, but its cast film prepared from chloroform solution showed endothermic DSC peaks probably due to the phase transition of the bilayer system in the presence of these solvents at 83, 33.1, and 29 °C, respectively. The thermal behavior of the cast film in 2-propanol was examined by the wavenumber shift of CH_2 stretching IR bands, which is associated with the trans−gauche conformational change of alkyl chains (Figure 1). At 18 °C in the first run, the as-prepared W_{10}/DODMA film in 2-propanol exhibited the antisymmetric and symmetric CH_2 stretching IR bands at 2919.5 and 2850.4 cm^{-1}, respectively, indicating that the alkyl chains of DODMA in the cast film have trans conformation preferentially.[23,24] Upon the temperature rise, a drastic upward shift was observed due to an increase in content of gauche conformation in the alkyl chains. It should be noted that the mid temperature of the shift (around 30 °C) agrees quite well with the phase transition temperature (29 °C) in the DSC measurement. Upon cooling to 10 °C (the starting points of the second run), both bands appeared at wavenumbers lower than those in the first run, indicating that the heating/cooling treatment caused the trans

(19) Chemseddine, A.; Sanchez, C.; Livage, J.; Launay, J. P.; Fournier, M. *Inorg. Chem.* **1984**, *23*, 2609.
(20) Ternes, S. C.; Pope, M. T. *Inorg. Chem.* **1978**, *17*, 500.
(21) Meldrum, F. C.; Kotov, N. A.; Fendler, J. H. *Chem. Mater.* **1995**, *7*, 1112.
(22) Fuchs, V. J.; Hartl, H,; Schiller, W.; Gerlach, U. *Acta Crystallogr.* **1976**, *B32*, 740.
(23) Cameron, D. G.; Casal, H. L.; Mantsh, H. H. *Biochemistry* **1980**, *19*, 3665.
(24) Nakashima, N.; Yamada, N.; Kunitake, T.; Umemura, J.; Takenaka, T. *J. Phys. Chem.* **1986**, 3374.

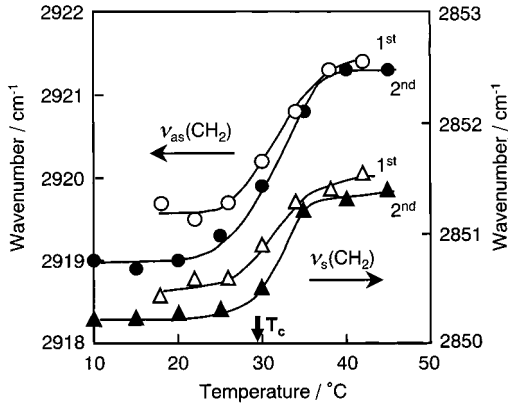

Figure 1. Temperature dependence of the wavenumber of CH_2 stretching IR bands ($\nu_{as}(CH_2)$, circle; $\nu_s(CH_2)$, triangle) of W_{10}/DODMA film in the presence of 2-propanol. Open and closed symbols indicate the first and second runs, respectively.

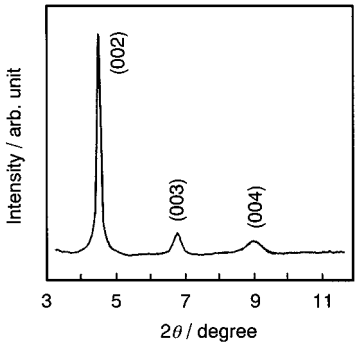

Figure 2. XRD pattern of W_{10}/DODMA cast film.

content to increase and therefore the DODMA molecules to become more oriented. Upon heating in the second run, the transition was also observed at around 30 °C. From these results, it can be concluded that the cast film of the W_{10}/DODMA ion complex possesses the typical thermal characteristic of the bilayer system that occurs in the phase transition of gel to liquid crystal associated with the trans−gauche conformational change of alkyl chains with keeping of the layered structure.[24−26]

The periodicity of the bilayer structure in the film was investigated by XRD measurements. The cast film of the W_{10}/TBA ion complex was X-ray amorphous, but that of W_{10}/DODMA showed distinct (00*L*) Bragg peaks of $L = 2$, 3, and 4, indicating that the film has a well-organized multibilayer structure (Figure 2). The basal plane spacing (*d*) of the films was 39 Å, which was larger than that of the original DODMA film (36 Å).[25] Considering the exchange of Br^- ions in the original DODMA film with larger $W_{10}O_{32}^{4-}$ cluster ions and the decline (orientation) of DODMA molecules in the film, it would be reasonable that $W_{10}O_{32}^{4-}$ ions are arranged two-dimensionally in the hydrophilic interlayers of the bilayer. The cross-sectional area of $W_{10}O_{32}^{4-}$ (ca. 96 Å^2), which is calculated by the product of lengths of its long and short axes,[22] almost fits with twice that of DODMA (54 Å^2).[27] A possible layered structure to satisfy the geometric condition and charge neutralization is that

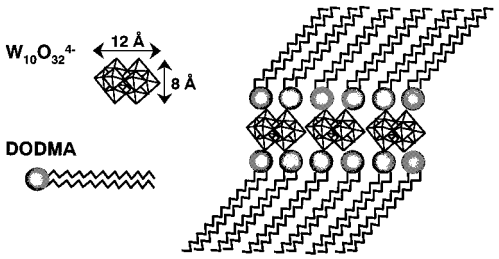

Figure 3. Schematic illustration of a possible structure of the W_{10}/DODMA composite.

one $W_{10}O_{32}^{4-}$ cluster ion is sandwiched between four monocationic DODMA molecules, two in the lower layer and the other two in the upper layer (Figure 3). Although the detailed information about the structure of the organic layers is not available, the structure of the hydrophilic part shown in Figure 3 is considered to be the most possible one at the present.

Photocatalytic Reaction with the W_{10}/DODMA System. When a quartz-supported cast film of W_{10}/DODMA was immersed in alcohol, such as ethanol and 2-propanol, and was exposed to UV light, the colorless film turned blue because of the reduction of W^{VI} to W^V and the appearance of the W^{VI}−W^V IVCT band with the absorption maximum at 630 nm. When W_{10}/DODMA-dispersed 2-propanol solution was exposed to the light of a 100-W Hg lamp in the presence of air, the white dispersed powder turned blue immediately and acetone, an oxidation product of 2-propanol, was produced in the solution. The formation of acetone was also observed under deoxidized conditions (N_2 atmosphere), but the color change and the acetone formation were never observed in the dark. It was reported that illumination of UV light to homogeneous CH_3CN−BuOH solution of W_{10}/TBA resulted in the prompt blue coloring and the formation of butylaldehyde as a consequence of photocatalytic dehydrogenation of BuOH by W_{10}/TBA.[28] With dehydrogenation of BuOH to the aldehyde under photoillumination, the decatungstate anion ($W_{10}O_{32}^{4-}$) changed to a protonated species ($H_2W_{10}O_{32}^{4-}$) in which two W ions out of ten were pentavalent.[28]

Figure 4 shows illumination−time courses of acetone formation in the W_{10}/DODMA−2-propanol system under aerobic (air) and anaerobic (N_2) conditions at 35 °C. Under anaerobic conditions, acetone formation reached saturation after 2 h and the amount was the same as that of dispersed W_{10}/DODMA within experimental error, indicating the occurrence of the stoichiometric reaction (1). In the presence of oxygen, on the other

$$(CH_3)_2CHOH + W_{10}O_{32}^{4-} \rightarrow (CH_3)_2CO + H_2W_{10}O_{32}^{4-} \quad (1)$$

hand, the amount of acetone increased almost linearly with increasing photoillumination time to a value that far exceeded the amount of charged W_{10}/DODMA, and the apparent turnover number at 3 h was about 20. This indicates that the photocatalytic reaction of oxidative dehydrogenation of 2-propanol proceeds in the presence of oxygen in which oxygen reoxidizes the protonated

(25) Kayjiyama, T.; Hamada, Y.; Kumamaru, F.; Takayanagi, M.; Okahata, Y.; Kunitake, T. *Rep. Prog. Polym. Phys. Jpn.* **1978**, *21*, 701.
(26) Fendler, J. H. *Membrane Mimetic Chemistry*; John Wiley & Sons: New York, 1982.
(27) The molecular area in the surface pressure−area isotherm of the DODMA monolayer was used as the molecular cross section.
(28) Yamase, T.; Takebayashi, N.; Kaji, M. *J. Chem. Soc., Dalton Trans.* **1984**, 793.

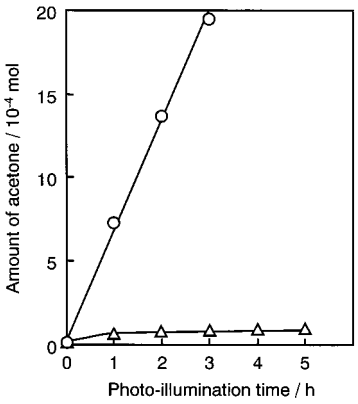

Figure 4. Photocatalytic reaction with W_{10}/DODMA for the oxidative dehydrogenation of 2-propanol into acetone in the presence of air (circle) or under a N_2 gas atmosphere (triangle) at 35 °C. 1×10^{-4} mol of W_{10}/DODMA was dispersed in 200 mL of 2-propanol and N_2 gas was purged for 0.5 h before photoillumination.

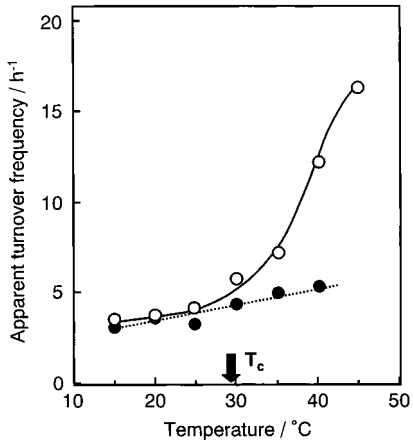

Figure 5. Temperature dependence of apparent turnover frequency of W_{10}/DODMA (open circle) and W_{10}/TBA (closed circle) for the oxidative dehydrogenation of 2-propanol into acetone in the presence of air.

species (reaction (2)) to complete the catalytic cycle.

$$H_2W_{10}O_{32}^{4-} + (^1/_2)O_2 \rightarrow W_{10}O_{32}^{4-} + H_2O \qquad (2)$$

Because the color of the catalysts remained blue during the reaction, it is likely that the reoxidation (2) of the catalyst is the rate-determining step.

Figure 5 shows temperature dependence of the photocatalytic oxidative dehydrogenation of 2-propanol under aerobic conditions. The amount of acetone increased dramatically above 29 °C, which is the phase-transition temperature (T_C) of the W_{10}/DODMA system; the values of turnover frequency at 40 and 45 °C were larger by a factor of 3−4 than that below T_C. Such a dramatic increase in the photocatalytic conversion of ethanol to acetoaldehyde was also observed around the phase-transition temperature (T_C = 33 °C) in the W_{10}/DODMA−ethanol system. When the W_{10}/TBA system, which did not show the phase transition in the temperature range examined (DSC), was used as the catalyst, the photocatalytic activity increased in a nearly straight fashion with an increase in temperature.

The above-mentioned results indicate that decatungstate ion ($W_{10}O_{32}^{4-}$) photocatalyzes the oxidative dehydrogenation of alcohol, even in the heterogeneous system, and that the overall reaction rate is controlled by the reoxidation step. The unique behavior of the W_{10}/DODMA system is that the reaction rate is controlled by the phase-transition property of the bilayer system. It is also noticed that the phase-transition property, which is usually observed in a bilayer cast film, is preserved in the powder of W_{10}/DODMA dispersed in alcohol. The relationship between the phase-transition behavior and the regulation of the reaction might be explained that the diffusion of reactant and/or products is more facile above T_C because the alkyl chains of DODMA are fluid above T_C while more rigid below T_C. Because the reoxidation step (2) is rate-determining, the diffusion of oxygen and/or water molecules must relate to the catalytic behavior regulated by the phase transition.

Photocatalytic Reaction with the W_{10}/Pt/DODMA System. In the case of photocalaysis with the W_{10}/DODMA mentioned above, oxygen is indispensable in reoxidizing the reduced species. The alternative to this is dehydrogenation accompanied by H_2 evolution. Here, the photocatalytic dehydrogenation of 2-propanol in the absence of oxygen to yield acetone and H_2 was investigated at 35 °C with a mixed system composed of W_{10}/DODMA and Pt nanoparticles (W_{10}/Pt/DODMA); the former plays a role in acetone formation as described, while the latter may assist the H_2 evolution reaction (3).

$$H_2W_{10}O_{32}^{4-} \rightarrow W_{10}O_{32}^{4-} + H_2 \qquad (3)$$

Pt nanoparticles were prepared by reducing the ion complex between DODMA and H_2PtCl_6 with formaldehyde and sodium hydroxide. The conversion of all the $PtCl_6^{2-}$ in the $PtCl_6$/DODMA complex into Pt was confirmed by the disappearance of UV absorption of $PtCl_6^{2-}$ below 250 nm for the chloroform solution. The composition of Pt/DODMA was determined to be Pt:DODMA = 1:2 by elementary analysis. Found (%): C, 66.15; H, 11.86; N, 2.04. Calcd (%) for Pt·$(DODMA^+)_2$: C, 66.71; H, 11.79; N, 2.05. The composition is consistent with the expected one from the electric neutrality of its precursor, $PtCl_6^{2-}/(DODMA^+)_2$. The Pt/DODMA powder did not show any XRD peaks indicating the layered structure. Instead, broad XRD peaks were observed at $2\theta = 39.8°$, 46.3°, and 67.5°, which are assignable to the diffraction from (111), (200), and (220) planes of cubic Pt crystal, respectively.[29] The average crystallite size of Pt in the Pt/DODMA composite was evaluated to be 55 Å by Scherrer's equation.[30] The three-component composites with various molar ratios (x) of [Pt]/[W_{10}], W_{10}/Pt[x]/DODMA, were prepared by dissolving W_{10}/DODMA and Pt/DODMA powders in chloroform, which was followed by evaporation.

In the W_{10}/DODMA−2-propanol system, the stoichiometric reaction (1) without H_2 evolution proceeded as already mentioned and again depicted in Figure 6. On the other hand, a trace amount of acetone was produced without H_2 evolution in the dispersed Pt/DODMA−2-propanol system; the Pt/DODMA did not dissolve in

(29) Swanson, T. *Natl. Bur. Stand. (U.S.), Circ.* **1953**, *539*, 131.
(30) The fwhm of the (111) diffraction peak was used for the calculation with Scherrer's equation ($d = 0.9\lambda/B \cos\theta$; d diameter of crystallite, λ wavelength of X-ray, B fwhm, and θ diffraction angle).

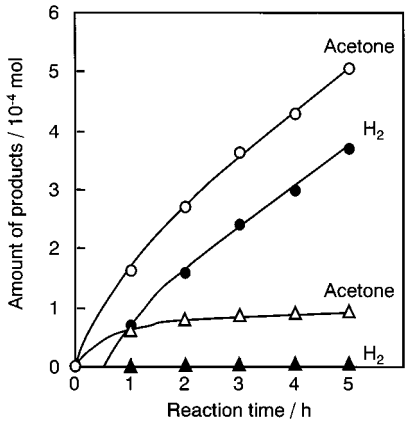

Figure 6. Time course of photocatalytic reactions of W_{10}/Pt-[0.3]/DODMA (circle) and W_{10}/DODMA (triangle) for the oxidative dehydrogenation of 2-propanol under a N_2 gas atmosphere at 35 °C. The catalysts containing 1×10^{-4} mol of $W_{10}O_{32}^{4-}$ were dispersed in 200 mL of 2-propanol and N_2 gas was purged for 0.5 h before photoillumination.

2-propanol. In contrast to these systems, the photo-assisted dehydrogenation of 2-propanol to acetone and H_2 proceeded catalytically with the W_{10}/Pt[x]/DODMA−2-propanol system ($x > 0$). As a representative example, the catalytic reaction with the W_{10}/Pt[0.3]/DODMA composite system at the temperature of 35 °C, which is higher than the phase-transition temperature of W_{10}/DODMA film (29 °C), is shown in Figure 6. The amounts of acetone and H_2 increased with increasing photoillumination time and the amount of acetone formed exceeded the amount of $W_{10}O_{32}^{4-}$ in W_{10}/Pt[0.3]/DODMA, even at 1 h with photoillumination, indicating that the catalytic cycle can proceed in the absence of oxygen for the W_{10}/Pt/DODMA composite system. The difference in amounts between acetone and H_2 gradually increased from 1.05×10^{-4} mol (1 h) to 1.40×10^{-4} mol (5 h), and the amounts of H_2 held in the catalyst were slightly larger than that of $W_{10}O_{32}^{4-}$ charged in the reaction medium (1×10^{-4} mol). This may suggest that decatungstate species are present in the form of protonated species ($H_2W_{10}O_{32}^{4-}$) during photocatalysis and the surplus H_2 seems to be accumulated on the surface of Pt as an adsorbed species (H_{ad}/Pt). It is also implied that the electron and proton transfer from $H_2W_{10}O_{32}^{4-}$ to Pt particles (4) and H_2 evolution from the surface of Pt particles (5) are the rate-determining steps of the catalytic reaction in the W_{10}/Pt/DODMA composite system. When W_{10}/DODMA and Pt/DODMA were separately dispersed in 2-propanol, on the other hand, the acetone formation was saturated within 2 h without H_2 evolution, showing the occurrence of the stoichiometric reaction (2). It can thus be concluded that Pt particles should be present in close vicinity to or in contact with decatungstate species to facilitate the reoxidation of $H_2W_{10}O_{32}^{4-}$ to $W_{10}O_{32}^{4-}$ and that such a situation is realized in the W_{10}/Pt/DODMA composite system, which is prepared by evaporating a chloroform solution of W_{10}/DODMA and Pt/DODMA. The photocatalytic cycle of the dehydrogenation of 2-propanol with the cooperation of decatungstate and Pt can be illustrated as in Figure 7.

$$H_2W_{10}O_{32}^{4-} \rightarrow W_{10}O_{32}^{4-} + 2H_{ad}/Pt \quad (4)$$

$$2H_{ad}/Pt \rightarrow H_2 \quad (5)$$

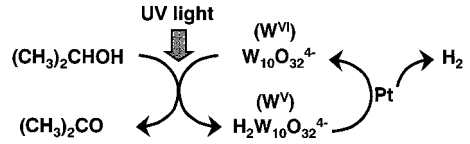

Figure 7. Catalytic cycle of the dehydrogenation of 2-propanol to acetone with W_{10}/Pt[x]/DODMA.

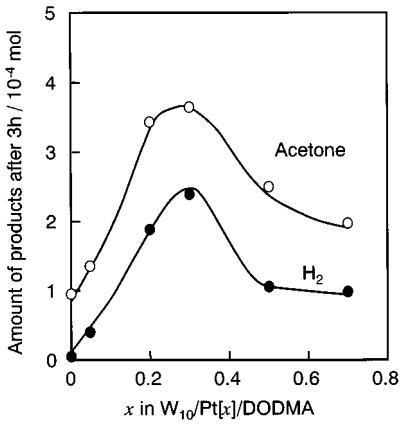

Figure 8. Photocatalytic dehydrogenation activity of W_{10}/Pt[x]/DODMA as a function of x. The reaction conditions were the same as those in Figure 6.

The efficiency of the cooperative catalysis depended on the molar ratio of [Pt]/[$W_{10}O_{32}^{4-}$], x, in the W_{10}/Pt[x]/DODMA, and the composite with $x = 0.3$ was the most active, as shown in Figure 8. In the present experiment, the amount of $W_{10}O_{32}^{4-}$ (W_{10}) present in the reaction system remained constant in the whole range of x examined. In the case that increasing x simply brings about an increase in the number of the contact points between W_{10} and Pt particles, a monotonic increase in the product formation with x would be expected. In another imaginary case that there is a solubility limit of the nonbilayer Pt/DODMA composite into the bilayer W_{10}/DODMA composite and the surplus Pt/DODMA exists as separate particles, the activity would be constant above the x value of the solubility limit. Therefore, the activity deterioration at $x > 0.3$ is possibly ascribable to the poor contact between W_{10} and Pt, which is caused by the structural change of the W_{10}/Pt/DODMA composite. Because Pt/DODMA does not form the bilayer structure as described, the incorporation of too much Pt may destroy the bilayer structure of W_{10}/Pt/DODMA and therefore the two-dimensional, nearly closed packing of W_{10} ions. Another possibility may be concerned with the importance of the two-dimensional packing of W_{10} ions in the W_{10}−Pt cooperative catalysis; the packing may be favorable for proton and electron transfer to the contact point of W_{10} and Pt from remote W_{10} ions. More detailed investigation on the structure and catalysis will be necessary to understand the W_{10}−Pt cooperative catalysis.

Conclusions

The present study demonstrated that the nanocomposite between decatungstate cluster ion and bilayer-forming amphiphile can be prepared by a simple ion-complexing method and it shows a unique photocatalytic property of decatungstate associated with the phase transition of the bilayer. It is also described that a

cooperative catalytic system between decatungstate and Pt nanoparticles can be fabricated by assembling them in a bilayer medium. The ion-complexing method can be extended to many kinds of polyoxometalate clusters and amphiphiles in principle, leading to new organic–inorganic nanosystems with unique functions.

Acknowledgment. This work was in part supported by Izumi Science and Technology Foundation. The study made use of instruments in the Center for Instrumental Analysis (XRD) of the Nagasaki University.

CM010007V